Dekan, Z., Sianati, S., Yousuf, A., Sutcliffe, K., Gillis, A., Mallet, C., Singh, P., Jin, A., Wang, A., Mohammadi, S., Stewart, M., Ratnayake, R., Fontaine, F., Lacey, E., Piggott, A., Du, Y., Canals, M., Sessions, R. B., Kelly, E. P., ... Christie, M. J. (2019). A tetrapeptide class of biased analgesics from an Australian fungus targets the -opioid receptor. *Proceedings of the National Academy of Sciences of the United States of America*, *116*(44), 22353-22358. https://doi.org/10.1073/pnas.1908662116

A tetrapeptide class of biased analgesics from an Australian fungus targets the μ-opioid receptor

Zoltan Dekan[a,1], Setareh Sianati[b,1], Arsalan Yousuf[b,1], Katy J. Sutcliffe[c,1], Alexander Gillis[b], Christophe Mallet[b,2], Paramjit Singh[a], Aihua H. Jin[a], Anna M. Wang[b], Sarasa A. Mohammadi[b], Michael Stewart[a], Ranjala Ratnayake[a], Frank Fontaine[a], Ernest Lacey[d], Andrew M. Piggott[a], Yan P. Du[b], Meritxell Canals[e,3], Richard B. Sessions[c], Eamonn Kelly[c], Robert J. Capon[a,4], Paul F. Alewood[a,4], and MacDonald J. Christie[b,4]

[a]Institute for Molecular Bioscience, The University of Queensland, 4072 Brisbane, Australia; [b]Discipline of Pharmacology, School of Medical Sciences, University of Sydney, NSW 2006, Australia; [c]Schools of Physiology, Pharmacology and Neuroscience, and Biochemistry, Biomedical Sciences Building, University of Bristol, BS8 1TD Bristol, United Kingdom; [d]Microbial Screening Technologies Pty. Ltd., Smithfield, NSW, 2164, Australia; and [e]Drug Discovery Biology Theme, Monash Institute of Pharmaceutical Sciences, Monash University, 3052 Parkville, Australia

Edited by Robert J. Lefkowitz, Howard Hughes Medical Institute, Duke University Medical Center, Durham, NC, and approved September 18, 2019 (received for review May 22, 2019)

An Australian estuarine isolate of *Penicillium* sp. MST-MF667 yielded 3 tetrapeptides named the bilaids with an unusual alternating LDLD chirality. Given their resemblance to known short peptide opioid agonists, we elucidated that they were weak (K_i low micromolar) μ-opioid agonists, which led to the design of bilorphin, a potent and selective μ-opioid receptor (MOPr) agonist (K_i 1.1 nM). In sharp contrast to all-natural product opioid peptides that efficaciously recruit β-arrestin, bilorphin is G protein biased, weakly phosphorylating the MOPr and marginally recruiting β-arrestin, with no receptor internalization. Importantly, bilorphin exhibits a similar G protein bias to oliceridine, a small nonpeptide with improved overdose safety. Molecular dynamics simulations of bilorphin and the strongly arrestin-biased endomorphin-2 with the MOPr indicate distinct receptor interactions and receptor conformations that could underlie their large differences in bias. Whereas bilorphin is systemically inactive, a glycosylated analog, bilactorphin, is orally active with similar in vivo potency to morphine. Bilorphin is both a unique molecular tool that enhances understanding of MOPr biased signaling and a promising lead in the development of next generation analgesics.

biased agonist | μ-opioid receptor | peptide drug | opioid analgesic | glycosylation

Developing ligands that target G protein-coupled receptors (GPCRs) in multiple functional states has attracted great interest, particularly with increasing knowledge of GPCR structure (1–3). These novel ligands are expected to underpin the development of agonists with superior pharmaceutically relevant properties, including biased receptor signaling (4, 5), whereby one downstream signaling pathway is favored over another. For example, biased agonists that signal by differentially recruiting G proteins over β-arrestin to the μ-opioid receptor (MOPr) could deliver better analgesics, based on the view that down-regulating β-arrestin recruitment diminishes adverse side effects (4, 6–8). Exploiting this concept, the G protein-biased MOPr agonist oliceridine (TRV130) is a potent analgesic in rodents, with lower respiratory depression and gastrointestinal dysfunction compared to morphine (7). Indeed, human clinical trials of oliceridine show reduced respiratory impairment compared to morphine administered at equi-analgesic doses (9). Reduced respiratory depression delivers improved safety, potentially reducing the burden of opioid overdoses, now at epidemic proportions in many jurisdictions (10).

Bioactive peptides display great promise for their novel pharmacological properties (11). Since the discovery of the relatively nonselective mammalian opioid peptides, the enkephalins, other endogenous mammalian ligands, including the tetrapeptide endomorphins that target the MOPr with high selectivity over the related κ-opioid (KOPr) and δ-opioid (DOPr) subtypes, have been found (12, 13). Natural peptide agonists containing a D-Ala in the second position formed by a posttranslational modification isolated from frog skin, dermorphin and deltorphin II, selectively target MOPr and DOPr, respectively (14). Similar synthetic modifications have yielded enhanced biological stability and receptor selectivity. For example, introduction of D-Ala stabilizes the enkephalins to proteolysis, and further substitutions yield highly stable, selective MOPr agonists such as DAMGO ([D-Ala2, *N*-MePhe4, Gly5-ol]-enkephalin) (15). However, to our knowledge, all endogenous opioid peptides acting on MOPr robustly recruit arrestins and produce MOPr internalization (16–19). Here, we report the discovery of 3 tetrapeptides, bilaids A–C (Fig. 1, [**1a-3a**]), from an Australian estuarine isolate of *Penicillium* sp. MST-MF667

Significance

Agonists of the μ-opioid receptor (MOPr) are currently the gold standard for pain treatment. However, their therapeutic usage is greatly limited by side effects including respiratory depression, constipation, tolerance, and dependence. Functionally selective MOPr agonists that mediate their effects preferentially through G proteins rather than β-arrestin signaling are believed to produce fewer side effects. Here, we present the discovery of 3 unusual tetrapeptides with a unique stereochemical arrangement of hydrophobic amino acids from an Australian estuarine isolate of *Penicillium* species. Building on these natural templates we developed bilorphin, a potent and selective highly G protein-biased agonist of the MOPr. Further, through the addition of a simple sugar moiety, we generated bilactorphin that is an effective analgesic in vivo.

Author contributions: Z.D., A.Y., A.G., C.M., A.M.W., S.A.M., M.C., R.B.S., E.K., R.J.C., P.F.A., and M.J.C. designed research; Z.D., S.S., A.Y., K.J.S., A.G., C.M., P.S., A.H.J., A.M.W., S.A.M., M.S., R.R., F.F., E.L., A.M.P., and Y.P.D. performed research; E.L. contributed new reagents/analytic tools; Z.D., S.S., A.Y., K.J.S., A.G., C.M., P.S., A.H.J., A.M.W., S.A.M., M.S., R.R., F.F., A.M.P., Y.P.D., M.C., R.B.S., E.K., R.J.C., P.F.A., and M.J.C. analyzed data; and Z.D., S.S., A.Y., K.J.S., A.G., S.A.M., M.C., R.B.S., E.K., R.J.C., P.F.A., and M.J.C. wrote the paper.

Competing interest statement: Patent Application(s) corresponding to Australian Patent Application 2018901944 The University of Sydney and The University of Queensland has been filed concerning this peptide. Title: Analgesics and Methods of Use Thereof.

This article is a PNAS Direct Submission.

[1]Z.D., S.S., A.Y., and K.J.S. contributed equally to this work.

[2]Present address: Neuro-Dol Basics & Clinical Pharmacology of Pain, INSERM, Université Clermont Auvergne, F-63000 Clermont-Ferrand, France.

[3]Present address: Centre of Membrane Proteins and Receptors, University of Nottingham, NG7 2UH Nottingham, United Kingdom.

[4]To whom correspondence may be addressed. Email: r.capon@imb.uq.edu.au, p.alewood@imb.uq.edu.au, or mac.christie@sydney.edu.au.

This article contains supporting information online at www.pnas.org/lookup/suppl/doi:10.1073/pnas.1908662116/-/DCSupplemental.

[initially reported as *P. bilaii* (20); maximum likelihood tree presented in *SI Appendix*, Fig. S1]. Discovery of the bilaids, which resemble known opioid peptides but featuring an unusual alternating sequence of antipodal amino acids (LDLD), led to our design of bilorphin (**3c**), a MOPr agonist, with G protein signaling bias similar to oliceridine. Bilorphin adopts a distinct conformational shape and intermolecular interactions in molecular dynamics (MD) simulations of the bilorphin–MOPr complex, consistent with predicted G protein bias at related GPCRs. Together with its in vitro and in vivo activity, we demonstrate that bilorphin provides a scaffold for the development of stable, orally active opioid peptides that are biased toward G protein signaling (**3g**).

Results

To date, the major opioid peptide families have only been detected in vertebrates (21). Through a broader screening program, we now report the discovery of 3 closely related tetrapeptides (Fig. 1), bilaids A (**1a,** FvVf-OH), B (**2a,** FvVy-OH), and C (**3a,** YvVf-OH), from the Australian estuarine-derived *Penicillium* sp. MST-MF667. Solvent extracts of cultivations of MST-MF667 were subjected to solvent partition followed by reversed-phase high-performance liquid chromatography (HPLC) to yield **1a** (0.15%), as well as traces of **2a** (0.0018%) and **3a** (0.0008%) (Fig. 1). The chemical structures for **1a–3a**, which resemble opioid peptides albeit with a unique, alternating LDLD amino acid configuration, were identified by spectroscopic analyses, chemical derivatization and degradation, and Marfey's analysis and total synthesis. In addition to synthesizing **1a–3a**, we prepared and screened a series of related analogs for inhibition of forskolin-induced cAMP formation in HEK cells expressing the human MOPr (hMOPr) (*SI Appendix*, Table S1). Five hits determined to be active at a concentration of 10 μM were tested for competitive binding against the hMOPr agonist [^{3}H]DAMGO. Bilaid C (**3a**) bound with the highest affinity at the hMOPr (K_i = 210 nM, Fig. 2*A* and *SI Appendix*, Table S1), consistent with the requirement for a Tyr moiety in the majority of peptide ligands targeting opioid receptors (22). Bilaid A (**1a**) showed more modest affinity (K_i = 3.1 μM) that was improved 4-fold through C-terminal amidation (K_i = 0.75 μM, **1e**), prompting us to apply this modification to further analogs. Analogs of bilaid A having a DLDL (**1b**, **1f**), LLDD (**1c**, **1g**), DDLL (**1d**), or LLLL (**1h**) configuration were generally inactive, with the exception of FVVF-NH_2 (**1h**), which weakly inhibited cAMP formation at 10 μM. These findings are consistent with previous SAR studies, which revealed that having L-amino acids in position 2, other than those that are Nα-alkylated (e.g., L-Pro), reduce opioid agonist activity

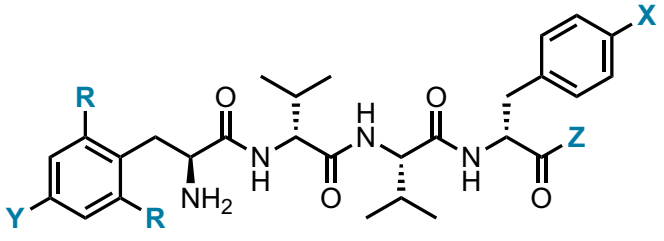

X	Y	Z	R
H	H	OH	H = bilaid A (**1a**)
OH	H	OH	H = bilaid B (**2a**)
H	OH	OH	H = bilaid C (**3a**)
H	OH	NH_2	Me = bilorphin (**3c**)
H	OH	L-Ser(β-Lac)-NH_2	Me = bilactorphin (**3g**)

Fig. 1. Structures of bilaids, bilorphin, and bilactorphin.

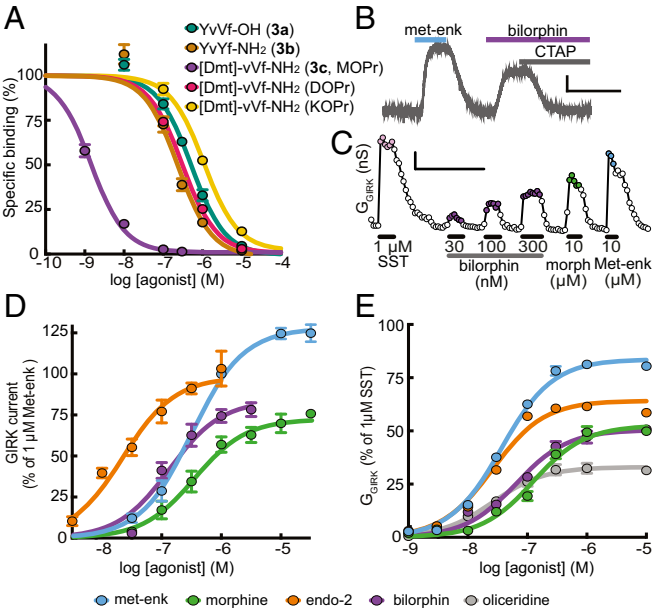

Fig. 2. (*A*) Competition for binding of [^{3}H]DAMGO to hMOPr (human recombinant MOPr) by the native bilaid YvVf-OH (**3a**), YvVf-NH_2 (**3b**) and bilorphin ([Dmt]vVf-NH_2) (**3c**), as well as bilorphin to hDOPr ([^{3}H]DADLE binding to human recombinant DOPr) and hKOPr ([^{3}H] U69593 binding to human recombinant KOPr). (*B*) Exemplar GIRK current recorded from a rat LC neuron in response to Met-enk (Met-enk; 1 μM), bilorphin (1 μM) applied for duration of bars shown, and its reversal by coapplication of the MOPr selective antagonist, CTAP (D-Phe-Cys-Tyr-D-Trp-Arg-Thr-Pen-Thr-NH_2, 1 μM). (Scale bars, 50 pA, 5 min.) (*C*) Exemplar record of bilorphin, morphine, and Met-enk–induced G_{GIRK} in mMOPr-expressing AtT20 cells in response to SST and opioids after alkylation of a fraction of receptors by the irreversible MOPr antagonist β-chlornaltrexamine (β-CNA). (Scale bar, 0.2 nS, 1 min.) (*D*) Agonist concentration–response relationships of opioids for activation of GIRK current in LC neurons normalized to 1 μM Met-enk applied first as a reference in each cell (n = 4–13 cells per data point; endo-2, endomorphin-2). (*E*) Concentration–response curves of G_{GIRK} induced by opioids in AtT20 cells after reducing the receptor reserve.

(23), as do D-amino acids in position 1 (24). Other bilaid analogs showed no MOPr activity at 10 μM.

C-terminal amidation of bilaid C (Fig. 2*A*, **3b** and *SI Appendix*, Table S1) improved hMOPr affinity (K_i = 93 nM), consistent with the increased binding of **1e** over **1a**. Dimethylation of the N-terminal tyrosine residue (**3c**) resulted in significantly increased potency (K_i = 1.1 nM), as has been observed for other opioid peptides (25). This compound, which we name bilorphin, bound with nearly 200-fold selectivity for hMOPr over hDOPr (K_i = 190 nM) and 700-fold selectivity over hKOPr (K_i = 770 nM) (Fig. 2*A* and *SI Appendix*, Table S1).

To assess functional activity of bilorphin, patch-clamp recordings of G protein-activated, inwardly rectifying potassium channel (GIRK) currents were made in rat locus coeruleus (LC) neurons, which natively express MOPr but not DOPr or KOPr (26). Bilorphin acted as an agonist with potency greater than morphine. Its actions were completely reversed by the highly MOPr selective antagonist CTAP (27) (n = 9, Fig. 2 *B* and *C* and *SI Appendix*, Table S1), establishing that bilorphin does not act on the closely related nociceptin or somatostatin (SST) receptors expressed by LC neurons (28). The native peptide, bilaid C, was 14-fold weaker than morphine in the same assay system (29). Bilaid C analogs with an acetylated N terminus (**3d**), or containing all L-amino acids (**3e** and **3f**), were inactive in LC neurons at 10–30 μM, confirming the importance of a free N terminus and the native LDLD motif for maintaining MOPr activity (*SI Appendix*, Table S1).

The relative potency and intrinsic efficacy of bilorphin in signaling pathways was examined in AtT20 cells stably expressing FLAG-tagged mouse MOPr (mMOPr) to enable bias analysis (Fig. 2 *C* and *E*). To reliably determine the relative intrinsic efficacy of bilorphin to activate G proteins (G_{GIRK}), we partially, irreversibly inactivated receptors to reduce the maximum response to the high efficacy natural agonist, Methionine5-enkephalin (Met-enk), to 80% of that produced by SST acting on native SST receptors in the same cells (Fig. 2 *C* and *E*). Maximal activation of SST receptors normally produces a G_{GIRK} increase equivalent to a maximal activation of MOPr (30). Under these conditions, bilorphin, morphine, and endomorphin-2 all displayed similar maximal responses. All agonists displayed similar potencies in the brain slice and cell assay, with the exception of Met-enk, the reduced potency of which in brain slices is known to result from its degradation by peptidases (31). As expected from brain slice experiments, all 3 opioids were moderately efficacious but less so than Met-enk (Fig. 2*E* and *SI Appendix*, Fig. S2*A*). In contrast, the G protein-biased, small molecule agonist oliceridine, activated G_{GIRK} significantly less efficaciously than either morphine or bilorphin (Fig. 2*E*).

MOPr C-terminal phosphorylation, β-arrestin recruitment, and internalization are thought to contribute to on-target opioid analgesic side effects so that G protein-biased opioids that avoid β-arrestin signaling should show an improved side effect profile (4, 7, 8). We therefore assayed the activity of bilorphin for inducing C-terminal phosphorylation, β-arrestin recruitment, and MOPr internalization in the same AtT20 cell line. Agonist-induced phosphorylation of residue serine 375 (Ser375) drives β-arrestin recruitment and internalization (32). We determined bilorphin-induced phosphoserine Ser375 (pSer375) phosphorylation using a phosphosite-specific antibody (Fig. 3 *A* and *D*) (33). Surprisingly, and unlike other opioid peptides (19, 32, 33), bilorphin produced low levels of pSer375 (30 μM, Fig. 3 *A* and *D* and *SI Appendix*, Fig. S2*B*), which appeared less than that produced by morphine, but this difference was not statistically significant (*SI Appendix*, Fig. S2*B*). Using MOPr-luciferase and β-arrestin 2-YFP constructs, a bioluminescence resonance energy transfer (BRET) assay was performed to determine β-arrestin 2 recruitment (Fig. 3 *B* and *D*) (34). Similar to phosphorylation, saturating concentrations of bilorphin induced very low levels of BRET efficiency, significantly less than that produced by morphine (30 μM, Fig. 3*B*). MOPr internalization was assessed immunocytochemically after 30 min of agonist treatment (Fig. 3 *C* and *D*). Bilorphin produced almost no detectable internalization of MOPr, compared to low levels induced by morphine and robust internalization driven by both endomorphin-2 and Met-enk (Fig. 3*D*). In summary, when normalized to the maximum response to Met-enk in each pathway, bilorphin displayed similar maximal G protein efficacy to morphine with progressive reduction in relative efficacy across pathways from Ser375 phosphorylation, β-arrestin recruitment to internalization (Fig. 3*D*), suggesting that bilorphin is a G protein-biased opioid.

Operational analysis, the de facto standard for quantifying biased signaling (35, 36), suggests that bilorphin is G protein biased relative to morphine (*SI Appendix*, Fig. S2) but this requires accurate determination of EC_{50}, which was impractical for bilorphin due to its very low internalization efficacy (*SI Appendix*, Fig. S2) (35). Calculation of relative efficacy from maximum response in each pathway provides a complementary estimate of bias in signaling assays where all agonists are partial (36, 37). This approach (*SI Appendix*, Fig. S2 and Table S2) substantiated the G protein bias of bilorphin relative to morphine (19, 34). To further substantiate the bias of bilorphin compared with morphine and the established G protein biased agonist oliceridine, both of which produce very little internalization, we enhanced internalization by overexpressing GRK2-YFP and β-arrestin 2-HA (38). In GRK2-positive cells, morphine, oliceridine, and

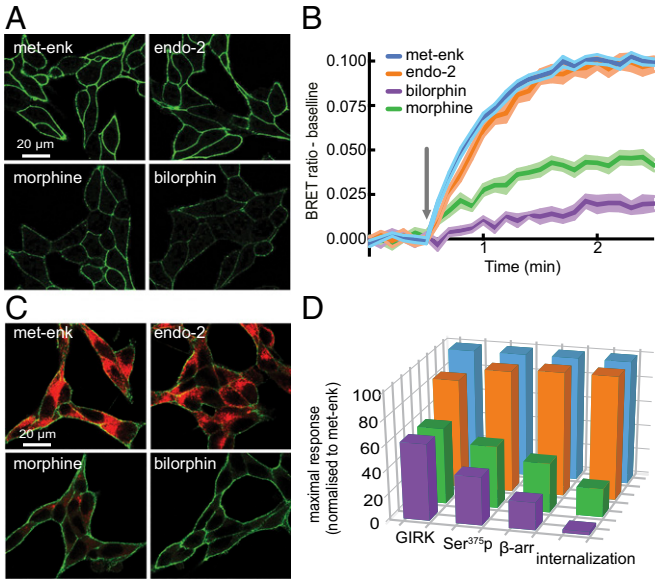

Fig. 3. (*A*) Representative images of S375 phosphorylation in AtT20 cells induced by saturating concentrations (30 μM) of Met-enk, endomorphin-2, morphine, and bilorphin after 5-min incubation. Colors enhanced uniformly for all images for presentation purposes. (*B*) Time course of ligand-induced BRET signal (ratio of emission of 535 nm/475 nm, baseline subtracted) indicating β-arrestin 2 recruitment after incubation with saturating concentrations of agonists (shown by the arrow). The band represents the SE of experiments repeated independently 6 times (each experiment in triplicate). (*C*) Example images of MOPr internalization 30 min after incubation with saturating concentrations of agonists. Dual staining was employed for quantification (membrane receptor in green and internalized receptor in red, colors enhanced uniformly for presentation purposes). (*D*) Maximal efficacy values of endomorphin-2, morphine and bilorphin relative to Met-enk for GIRK channel activation, Ser375 phosphorylation, β-arrestin 2 recruitment, and internalization (all normalized to Met-enk; nonnormalized data in *SI Appendix*, Fig. S2).

bilorphin all produced clear internalization signals (*SI Appendix*, Fig. S3*A*). Quantification shows that even under these amplified conditions, bilorphin induces similar MOPr internalization to oliceridine but significantly less than morphine at saturating concentrations (*SI Appendix*, Fig. S3 *B* and *C*). Calculation of bias relative to morphine with the ΔE_{Max} method suggests that bilorphin exhibits significant G protein bias that is similar to oliceridine, further establishing it to be a G protein biased opioid (*SI Appendix*, Fig. S3*C*).

The widely accepted mechanism for ligand bias is the stabilization of distinct GPCR conformations that favor coupling to different intracellular proteins (39). However, how such biased agonists interact with the receptor binding pocket and the nature of these biased receptor conformations, particularly for the MOPr, is poorly understood. To this end, we performed molecular docking and MD simulations (40) to compare possible biased receptor conformations of the G protein-biased bilorphin versus β-arrestin–biased endomorphin-2. First, we analyzed the predicted binding poses of bilorphin and endomorphin-2 after 1 μs of MD simulation to determine if interactions with the MOPr binding pocket could differentiate these oppositely biased compounds. The binding pose of bilorphin is shown in Fig. 4*A* and *SI Appendix*, Fig. S4*A* and that of endomorphin-2 in Fig. 4*B* and *SI Appendix*, Fig. S4*B*. There were similarities in how bilorphin and endomorphin-2 interacted with the MOPr; both peptides bound in the orthosteric pocket with the phenol groups of the Dmt (bilorphin) or Tyr1 (endomorphin-2) orientated toward the intracellular side of MOPr, and maintained interactions with $Asp147^{3.32}$, $Trp293^{6.48}$, and $His297^{6.52}$ (Fig. 4*C*). For the latter

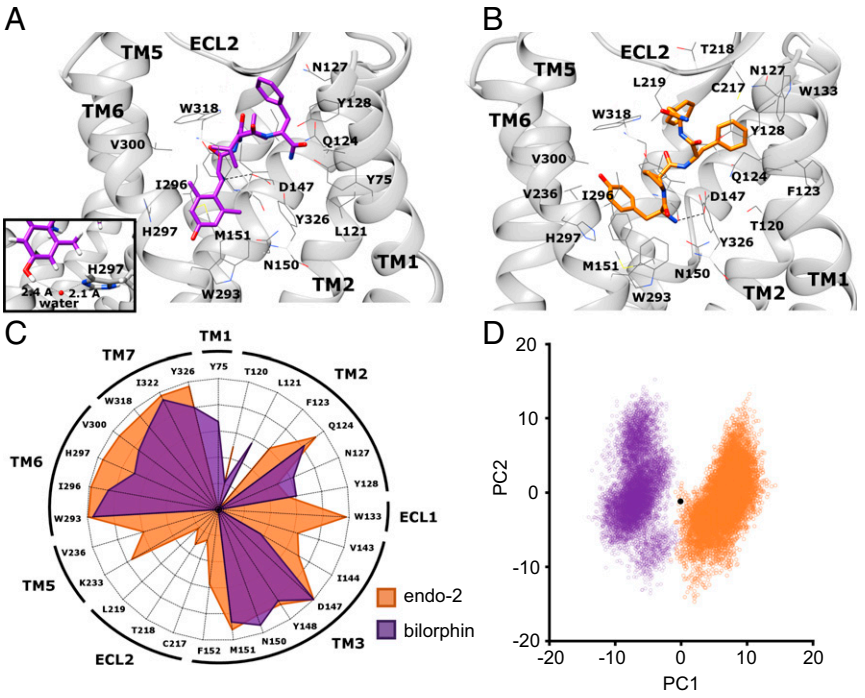

Fig. 4. Predicted binding poses of bilorphin (purple) (*A*) and endomorphin-2 (orange) (*B*), and the positions of the surrounding binding pocket residues (gray) obtained after molecular docking and 1 μs of MD simulations. The salt bridge between the protonated amine of the ligands and Asp147$^{3.32}$ is marked as a dashed black line. TM7 has been removed for clarity. (*C*) Ligand–residue interaction fingerprints for the bilorphin–MOPr complex (purple) and endomorphin2–MOPr complex (orange). Data are expressed as the percentage of simulation time each residue is within 4.5 Å of the ligand, with points radiating outwards from 0 to 100% in 20% increments. (*D*) Principal component analysis was performed on the alpha carbons of the receptor transmembrane domains, before projecting the receptor conformations at each simulation time point onto PC1 and PC2. The bilorphin–MOPr complex is in purple, the endomorphin-2–MOPr complex in orange, and the black point indicates the conformation of the inactive MOPr model to which the peptides were docked.

residue, bilorphin switched between a direct interaction and hydrogen bonding via a bridging water molecule (Fig. 4 *A*, *Inset*). However, there were also important differences in how these peptides interact with the MOPr binding pocket. For bilorphin, the rest of the tetrapeptide chain extended out toward the extracellular side of MOPr, making contacts with residues at the top of TMs 1, 2, and 7, resulting in bilorphin, but not endomorphin-2, interacting with Tyr75$^{1.39}$ in TM1. Conversely, endomorphin-2 extended toward ECL1 and ECL2 and the top of TM2. Endomorphin-2 therefore interacted with the extracellular loops, contacting W133^{ECL1} in ECL1 for the entire simulation time, and transiently interacting with Cys217^{ECL2}, Thr218^{ECL2}, and Leu219^{ECL2} of ECL2. Whereas, these interactions were absent for bilorphin. Moreover, endomorphin-2 made a greater number of contacts with residues in TM3 and TM5 than bilorphin.

These predicted binding poses were validated by root mean square deviation analysis showing stability of each ligand in the binding pocket (*SI Appendix*, Fig. S4 *C* and *D*), and our docking and MD protocol successfully recapitulated the binding pose of DAMGO when compared to the cryo-electron microscopy structure of the DAMGO-bound MOPr–Gi complex (*SI Appendix*, Fig. S5) (41).

Next, principal component analysis was employed to examine the overall conformational changes in the receptor transmembrane helices in the presence of bilorphin or endomorphin-2. The receptor conformations at each time point were projected onto principal components (PC) 1 and 2 and plotted in Fig. 4*D*. PC1 and PC2 accounted for 28.9% and 10.9% of the variance, respectively. Both peptide–MOPr complexes sampled conformations across PC2, but clustered differently based on PC1, suggesting that the MOPr adopted distinct conformations when bound to each biased agonist.

As depicted in *SI Appendix*, Fig. S4*E*, PC1 primarily described alternative conformations in the extracellular region of the receptor close to the orthosteric binding site and, to a lesser extent, differences in the intracellular portions of the helices. With endomorphin-2 bound, there was an overall contraction of the orthosteric site, due to inward movements of TMs 2, 3, 4, and 7. Whereas, with bilorphin bound, there was a bulging of the middle portion of TM1 and a shift outwards from the helix bundle, relative to the endomorphin-2–bound receptor. These alternative conformations of the helices were also reflected in the volume of the orthosteric site, as with bilorphin bound the binding pocket volume was on average 1.6 times greater than with endomorphin-2 bound (42) (*SI Appendix*, Fig. S4*F*). On the intracellular side of MOPr, PC1 described inward movements of TMs 5, 6, and 7 with endomorphin-2 bound, compared to the bilorphin-bound MOPr (*SI Appendix*, Fig. S4*E*). The result was a more occluded intracellular cavity in the endomorphin-2–bound MOPr, compared to that with bilorphin bound.

Analysis of the MD data therefore suggests that the different ligand–residue interactions for these oppositely biased peptides (with respect to the extracellular loops and TM1) may lead to the alternative receptor conformations described by the principal component analysis and, hence, the opposing bias profiles of bilorphin and endomorphin-2.

We then evaluated bilorphin in vivo. Bilorphin failed to inhibit nociception in the hotplate test in mice when administered subcutaneously (s.c.) (100 mg/kg, $n = 4$) or intravenously (i.v.) (50 mg/kg $n = 4$). By contrast, bilorphin was antinociceptive after intrathecal injection (5 nmol per mouse, peak effect 41 ± 9% MPE $n = 4$, versus 0 ± 1.5% for vehicle, $n = 4$), suggesting the lack of systemic activity is due to poor penetration of the blood–brain barrier (BBB). We therefore developed several bilorphin analogs with substitutions thought to enhance BBB permeability, including glycosylation near the C terminus (43). The diglycosylated analog, bilactorphin (**3g**), was a potent analgesic after systemic administration (s.c; ED_{50} of 34 μmol/kg, 95% confidence interval [CI] = 28–40 μmol/kg; *SI Appendix*, Fig. S6 *A* and *B*), was nearly equipotent with morphine (ED_{50} of 27 μmol/kg, 95% CI = 24–30 μmol/kg *SI Appendix*, Fig. S6*B*) and was antagonized by coadministration of the opioid antagonist, naltrexone (*SI Appendix*, Fig. S6*A*). Bilactorphin was also active after i.v. (peak effect of 88.9 ± 11.8 versus 14.4 ± 1.8% MPE for vehicle, $n = 3$–4) or oral administration (*SI Appendix*, Fig. S7). In contrast, the monoglycosylated analog **3h** was systemically inactive, consistent with previous modified opioid peptides (43). These findings establish that the natural LDLD opioid peptide backbone we have

discovered is a viable framework for development of G protein-biased opioid analgesics. Like bilorphin, bilactorphin was a potent partial opioid agonist of G proteins in AtT20 cells but exhibited a small loss of potency compared with bilorphin (*SI Appendix*, Fig. S6 *C* and *D*). Bilactorphin did, however, display increased internalization and β-arrestin recruitment compared to bilorphin (*SI Appendix*, Fig. S6 *E* and *F*) and thus might not be suitable for directly testing the role of bias in opioid side-effect profile. Alternative modifications that do not disrupt G protein bias of the parent bilorphin might be better suited to enhance BBB permeability.

Discussion

Nature has inspired many of the most well-known and widely used analgesics, from natural salicin in willow (*Salix*) bark to synthetic aspirin, from opioid poppy alkaloids such as morphine and codeine to synthetic hydrocodone (Vicodin), oxycodone (OxyContin), and buprenorphine (Subutex). Notwithstanding their value in alleviating pain, serious adverse side effects, combined with the challenge of addiction, abuse, and acquired tolerance, render these analgesics (particularly opioids) far from ideal. There is an urgent need to discover and develop new, safer and more efficacious analgesics, with mechanisms of actions that mitigate against risk.

We therefore investigated the analgesic potential of a class of tetrapeptides, the bilaids (**1a–3a**), isolated from a *Penicillium* fungus. Taking advantage of an unprecedented natural scaffold comprising alternating LDLD configuration amino acids, which imparts inherent biostability, we designed a peptide-based G protein-biased MOPr agonist, bilorphin (**3c**). Furthermore, we assembled proof-of-concept data that this pharmacophore can be optimized to yield an orally active MOPr agonist analgesic, bilactorphin (**3g**).

G protein-biased opioid agonists have been proposed as a route to improving therapeutic profile (4, 7, 8). Among known peptide opioid agonists, which typically are biased toward β-arrestin signaling relative to morphine (19, 34), the pharmacological profile of bilorphin is most unusual, although a synthetic opioid cyclopeptide with G protein bias was recently reported (44). Bilorphin enjoys an opioid signaling bias comparable to oliceridine, a G protein-biased drug candidate in phase III clinical trials. Glycosylation of bilorphin produced an analog active in vivo via s.c. and oral administration, validating the bilorphin tetrapeptide backbone as a platform for further development of druggable signaling-biased opioid agonists. Preclinical development of other G protein-biased agonists shows a favorable profile with reduced respiratory depression and constipation. The first such compound to reach clinical trials, oliceridine, was reported to have an increased therapeutic window between antinociceptive and respiratory depressive activity (7) and appears to be safer in humans than morphine for equi-analgesic doses (9). Similarly, a series of substituted fentanyl analogs was observed to produce an increased therapeutic window for respiratory depression in mice, correlating with increased G protein versus β-arrestin 2 recruitment (8).

To investigate whether bias could be explained by the differential interaction of bilorphin and endomorphin-2 with MOPr, or by distinct receptor conformational changes initiated by each, we undertook MD simulations with bilorphin and compared this to the arrestin-biased opioid, endomorphin-2, bound to MOPr. Both peptides were docked to the orthosteric binding site of MOPr and displayed differences in ligand–residue interactions, which may translate to their differing bias profiles. Notably, endomorphin-2 transiently interacted with residues in ECL1 and ECL2, including the conserved residue Leu219, proposed to be important for arrestin-bias and ligand residence time at the 5-HT_{2A} and 5-HT_{2B} receptors and other aminergic GPCRs (45, 46). The cryo-electron microscopy–resolved structure of the DAMGO–MOPr–G_i complex also showed DAMGO, which robustly recruits arrestin, interacting with the receptor extracellular loops (41). In contrast, bilorphin did not contact the extracellular loops and instead interacted with TM1. Intriguingly, the extracellular end of TM1 has also been identified as part of the binding pocket for the G protein-biased GLP-1 agonist, ExP5 (47) and, in addition, has been implicated in the allosteric communication between the binding site and intracellular domain for oliceridine at the MOPr (48). Moreover, the interactions between the peptides and the MOPr binding pocket appear to translate to the divergent conformational changes observed by principal component analysis, resulting in the MOPr adopting a distinct conformation with bilorphin bound compared to endomorphin-2. Specifically, with bound endomorphin-2, the extracellular portions of the transmembrane domains moved inwards so that the orthosteric binding pocket contracted relative to the bilorphin-bound MOPr. On the intracellular side of the receptor TM5, 6, and 7 adopted distinct positions depending on the bound peptide, mainly an inward shift of these helices in the presence of endormorphin-2, resulting in a more occluded intracellular cavity for this arrestin-biased ligand. Of interest, this is in line with the proposed binding pocket for arrestins at the base of the GPCR being slightly smaller than those for G proteins (49, 50).

While it remains challenging at present to associate ligand-induced GPCR conformations with differential coupling to G proteins or arrestins, particularly in the absence of a large structurally diverse panel of biased MOPr agonists, the subtle differences in ligand–residue interactions and conformations of the MOPr helices that we have modeled here may represent the initial changes induced by the oppositely biased peptides, bilorphin and endomorphin-2. These different interactions and MOPr conformations may well lead to the different signaling profiles reported for these biased peptide agonists at MOPr.

It remains uncertain, however, whether G protein bias per se is the sole property contributing to the improved safety of new opioid drugs such as oliceridine (9). Using receptor knockdown, we have shown here that oliceridine has very low G protein efficacy compared with morphine, similar to findings using receptor depletion with a cAMP assay system (37). Similar low efficacy results have recently been reported for another opioid, PZM21, also claimed to be safer than morphine (4, 51). Furthermore, it is difficult to evaluate maximal G protein efficacy of novel biased agonists in other studies because assays were insensitive to the relatively low G protein efficacy of morphine (7, 8). Very low G protein efficacy may indeed be a confounding factor in the preclinical and clinical studies of side effect profile, given that other agonists with very low G protein efficacy such as buprenorphine are not strongly G protein biased (19) but are well characterized to produce less respiratory depression, and overdose death than highly efficacious agonists such as morphine and methadone (52). Because bilorphin is strongly G protein biased and has nearly equivalent maximal G protein efficacy to morphine, further development of BBB penetrant analogs that can release the parent molecule will facilitate direct test of the influence of bias without being confounded by differing G protein efficacy.

Finally, we have elucidated an analgesic pharmacophore based on the discovery of the bilaids and related bilorphin and bilactorphin motifs. Unusually, they derive from a microbial source, an untapped resource for analgesics and worthy of further investigation. This observation suggests that microbes may be an untapped resource for new analgesics, deserving of further investigation.

Experimental Procedures. Full details on the materials and methods used are available in *SI Appendix*. Solvent extracts solid phase cultivations of MST-MF667 were subjected to solvent partition followed by reversed-phase HPLC, and chemical structures were identified on the basis of detailed spectroscopic analysis, chemical derivatization and degradation, Marfey's

analysis and total synthesis. All peptides were assembled manually by stepwise solid-phase peptide synthesis. MOPr activity was initially screened using competition opioid radioligand binding to membranes from cultured cells expressing hMOPr, hDOPr, or hKOPr receptors, then agonist activity screened at hMOPr using inhibition of forskolin-stimmulated cAMP formation. Agonist activation of MOPr-coupled GIRK channels was then quantified using superfusion onto LC neurons in rate brain slices using whole-cell patch clamp recording. Signaling pathway analysis was quantified in AtT20 cells stably expressing mMOPr using perforated patch recording for GIRK channels activation (G protein signal), fluorescence immunohistochemistry for Ser375 phosphorylation and MOPr internalization and arrestin recruitment with a BRET-based approach. Molecular docking was performed using the Bristol University Docking Engine (53). The selected peptide–MOPr complexes were then embedded in a lipid and cholesterol bilayer and used in all-atom MD simulations. Multiple simulations (8×125 ns), with different initial velocities, were performed under the Amber ff14SB and Lipid14 forcefields, to yield a total of 1 μs of trajectory data for each peptide. Behavioral assays of analgesia were performed using the hotplate latency assay in mice. Statistical analyses were performed as described in *SI Appendix*. All values are expressed as means ± SEM, except where noted otherwise (*SI Appendix*, Fig. S2).

ACKNOWLEDGMENTS. This work was supported by Program Grant APP1072113 from the National Health and Medical Research Council of Australia (to P.F.A. and M.J.C.).

1. A. Manglik *et al.*, Crystal structure of the μ-opioid receptor bound to a morphinan antagonist. *Nature* **485**, 321–326 (2012).
2. W. Huang *et al.*, Structural insights into μ-opioid receptor activation. *Nature* **524**, 315–321 (2015).
3. J. J. Liu, R. Horst, V. Katritch, R. C. Stevens, K. Wüthrich, Biased signaling pathways in β2-adrenergic receptor characterized by 19F-NMR. *Science* **335**, 1106–1110 (2012).
4. A. Manglik *et al.*, Structure-based discovery of opioid analgesics with reduced side effects. *Nature* **537**, 185–190 (2016).
5. J. S. Smith, R. J. Lefkowitz, S. Rajagopal, Biased signalling: From simple switches to allosteric microprocessors. *Nat. Rev. Drug Discov.* **17**, 243–260 (2018).
6. K. M. Raehal, J. K. Walker, L. M. Bohn, Morphine side effects in beta-arrestin 2 knockout mice. *J. Pharmacol. Exp. Ther.* **314**, 1195–1201 (2005).
7. S. M. DeWire *et al.*, A G protein-biased ligand at the μ-opioid receptor is potently analgesic with reduced gastrointestinal and respiratory dysfunction compared with morphine. *J. Pharmacol. Exp. Ther.* **344**, 708–717 (2013).
8. C. L. Schmid *et al.*, Bias factor and therapeutic window correlate to predict safer opioid analgesics. *Cell* **171**, 1165–1175.e13 (2017).
9. N. Singla *et al.*, A randomized, Phase IIb study investigating oliceridine (TRV130), a novel μ-receptor G-protein pathway selective (μ-GPS) modulator, for the management of moderate to severe acute pain following abdominoplasty. *J. Pain Res.* **10**, 2413–2424 (2017).
10. D. Dowell, R. K. Noonan, D. Houry, Underlying factors in drug overdose deaths. *JAMA* **318**, 2295–2296 (2017).
11. I. W. Hamley, Small bioactive peptides for biomaterials design and therapeutics. *Chem. Rev.* **117**, 14015–14041 (2017).
12. J. E. Zadina, L. Hackler, L. J. Ge, A. J. Kastin, A potent and selective endogenous agonist for the mu-opiate receptor. *Nature* **386**, 499–502 (1997).
13. J. T. Williams, M. J. Christie, O. Manzoni, Cellular and synaptic adaptations mediating opioid dependence. *Physiol. Rev.* **81**, 299–343 (2001).
14. G. Kreil, Peptides containing a D-amino acid from frogs and molluscs. *J. Biol. Chem.* **269**, 10967–10970 (1994).
15. D. Roemer *et al.*, A synthetic enkephalin analogue with prolonged parenteral and oral analgesic activity. *Nature* **268**, 547–549 (1977).
16. G. L. Thompson *et al.*, Biased agonism of endogenous opioid peptides at the μ-opioid receptor. *Mol. Pharmacol.* **88**, 335–346 (2015).
17. P. Molinari *et al.*, Morphine-like opiates selectively antagonize receptor-arrestin interactions. *J. Biol. Chem.* **285**, 12522–12535 (2010).
18. G. Rivero *et al.*, Endomorphin-2: A biased agonist at the μ-opioid receptor. *Mol. Pharmacol.* **82**, 178–188 (2012).
19. J. McPherson *et al.*, μ-opioid receptors: Correlation of agonist efficacy for signalling with ability to activate internalization. *Mol. Pharmacol.* **78**, 756–766 (2010).
20. R. J. Capon, M. Stewart, R. Ratnayake, E. Lacey, J. H. Gill, Citromycetins and bilains A-C: New aromatic polyketides and diketopiperazines from Australian marine-derived and terrestrial Penicillium spp. *J. Nat. Prod.* **70**, 1746–1752 (2007).
21. G. Sundström, S. Dreborg, D. Larhammar, Concomitant duplications of opioid peptide and receptor genes before the origin of jawed vertebrates. *PLoS One* **5**, e10512 (2010).
22. A. S. Horn, J. R. Rodgers, Structural and conformational relationships between the enkephalins and the opiates. *Nature* **260**, 795–797 (1976).
23. R. Schmidt *et al.*, Structure-activity relationships of dermorphin analogues containing N-substituted amino acids in the 2-position of the peptide sequence. *Int. J. Pept. Protein Res.* **46**, 47–55 (1995).
24. J. S. Morley, Structure-activity relationships of enkephalin-like peptides. *Annu. Rev. Pharmacol. Toxicol.* **20**, 81–110 (1980).
25. G. M. Zhao, X. Qian, P. W. Schiller, H. H. Szeto, Comparison of [Dmt1]DALDA and DAMGO in binding and G protein activation at mu, delta, and kappa opioid receptors. *J. Pharmacol. Exp. Ther.* **307**, 947–954 (2003).
26. R. A. North, J. T. Williams, A. Surprenant, M. J. Christie, Mu and delta receptors belong to a family of receptors that are coupled to potassium channels. *Proc. Natl. Acad. Sci. U.S.A.* **84**, 5487–5491 (1987).
27. J. T. Pelton, W. Kazmierski, K. Gulya, H. I. Yamamura, V. J. Hruby, Design and synthesis of conformationally constrained somatostatin analogues with high potency and specificity for mu opioid receptors. *J. Med. Chem.* **29**, 2370–2375 (1986).
28. M. Connor, C. W. Vaughan, B. Chieng, M. J. Christie, Nociceptin receptor coupling to a potassium conductance in rat locus coeruleus neurones in vitro. *Br. J. Pharmacol.* **119**, 1614–1618 (1996).
29. M. Sadeghi, T. M. Tzschentke, M. J. Christie, μ-Opioid receptor activation and noradrenaline transport inhibition by tapentadol in rat single locus coeruleus neurons. *Br. J. Pharmacol.* **172**, 460–468 (2015).
30. A. Yousuf *et al.*, Role of phosphorylation sites in desensitization of μ-opioid receptor. *Mol. Pharmacol.* **88**, 825–835 (2015).
31. J. T. Williams, M. J. Christie, R. A. North, B. P. Roques, Potentiation of enkephalin action by peptidase inhibitors in rat locus ceruleus in vitro. *J. Pharmacol. Exp. Ther.* **243**, 397–401 (1987).
32. R. El Kouhen *et al.*, Phosphorylation of Ser363, Thr370, and Ser375 residues within the carboxyl tail differentially regulates mu-opioid receptor internalization. *J. Biol. Chem.* **276**, 12774–12780 (2001).
33. C. Doll *et al.*, Agonist-selective patterns of μ-opioid receptor phosphorylation revealed by phosphosite-specific antibodies. *Br. J. Pharmacol.* **164**, 298–307 (2011).
34. G. L. Thompson *et al.*, Systematic analysis of factors influencing observations of biased agonism at the mu-opioid receptor. *Biochem. Pharmacol.* **113**, 70–87 (2016).
35. T. Kenakin, Measurement of receptor signaling bias. *Curr. Protoc. Pharmacol.* **74**, 2.15.1–2.15.15 (2016).
36. E. Kelly, Efficacy and ligand bias at the μ-opioid receptor. *Br. J. Pharmacol.* **169**, 1430–1446 (2013).
37. J. Burgueño *et al.*, A complementary scale of biased agonism for agonists with differing maximal responses. *Sci. Rep.* **7**, 15389 (2017).
38. J. Zhang *et al.*, Role for G protein-coupled receptor kinase in agonist-specific regulation of mu-opioid receptor responsiveness. *Proc. Natl. Acad. Sci. U.S.A.* **95**, 7157–7162 (1998).
39. T. Kenakin, Functional selectivity and biased receptor signaling. *J. Pharmacol. Exp. Ther.* **336**, 296–302 (2011).
40. K. J. Sutcliffe, G. Henderson, E. Kelly, R. B. Sessions, Drug binding poses relate structure with efficacy in the μ opioid receptor. *J. Mol. Biol.* **429**, 1840–1851 (2017).
41. A. Koehl *et al.*, Structure of the μ-opioid receptor-G_i protein complex. *Nature* **558**, 547–552 (2018).
42. J. Dundas *et al.*, CASTp: Computed atlas of surface topography of proteins with structural and topographical mapping of functionally annotated residues. *Nucleic Acids Res.* **34**, W116–W118 (2006).
43. Y. Li *et al.*, Opioid glycopeptide analgesics derived from endogenous enkephalins and endorphins. *Future Med. Chem.* **4**, 205–226 (2012).
44. J. Piekielna-Ciesielska, F. Ferrari, G. Calo', A. Janecka, Cyclopeptide Dmt-[D-Lys-p-CF_3-Phe-Phe-Asp]NH_2, a novel G protein-biased agonist of the mu opioid receptor. *Peptides* **101**, 227–233 (2018).
45. D. Wacker *et al.*, Crystal structure of an LSD-bound human serotonin receptor. *Cell* **168**, 377–389.e12 (2017).
46. J. D. McCorvy *et al.*, Structure-inspired design of β-arrestin-biased ligands for aminergic GPCRs. *Nat. Chem. Biol.* **14**, 126–134 (2018).
47. Y. L. Liang *et al.*, Phase-plate cryo-EM structure of a biased agonist-bound human GLP-1 receptor-Gs complex. *Nature* **555**, 121–125 (2018).
48. S. Schneider, D. Provasi, M. Filizola, How oliceridine (TRV-130) binds and stabilizes a μ-opioid receptor conformational state that selectively triggers G protein signaling pathways. *Biochemistry* **55**, 6456–6466 (2016).
49. J. Okude *et al.*, Identification of a conformational equilibrium that determines the efficacy and functional selectivity of the μ-opioid receptor. *Angew. Chem. Int. Ed. Engl.* **54**, 15771–15776 (2015).
50. B. Carpenter, C. G. Tate, Active state structures of G protein-coupled receptors highlight the similarities and differences in the G protein and arrestin coupling interfaces. *Curr. Opin. Struct. Biol.* **45**, 124–132 (2017).
51. R. Hill *et al.*, The novel μ-opioid receptor agonist PZM21 depresses respiration and induces tolerance to antinociception. *Br. J. Pharmacol.* **175**, 2653–2661 (2018).
52. B. Mégarbane, R. Hreiche, S. Pirnay, N. Marie, F. J. Baud, Does high-dose buprenorphine cause respiratory depression?: Possible mechanisms and therapeutic consequences. *Toxicol. Rev.* **25**, 79–85 (2006).
53. S. McIntosh-Smith, J. Price, R. B. Sessions, A. A. Ibarra, High performance *in silico* virtual drug screening on many-core processors. *Int. J. High Perform. Comput. Appl.* **29**, 119–134 (2015).